This article has been accepted for publication in a future issue of this journal, but has not been fully edited. Content may change prior to final publication. Citation information: DOI 10.1109/LPT.2018.2883211, IEEE Photonics Technology Letters

Comparing Laser Hybrid-Integration and Fiber Coupling with Standard Grating Couplers on Si-PICs

L. Zagaglia, F. Floris, L. Carroll, and P. O'Brien

***Abstract*—We compare the simulated optical insertion-losses and fabrication-tolerances of a micro-optical bench (MOB) for laser hybrid-integration on the 220nm Silicon-on-Insulator (SOI) photonic-platform to standard fiber-to-grating coupling. Our millimeter-scale two-dimensional finite difference time domain (2D-FDTD) simulation captures (i) aberration, (ii) reflection, (iii) diffraction, and (iv) wave-guiding effects in a single-shot and completely self-consistent way, indicating that light from a laser-diode can be coupled to the SOI photonic integrated circuit (PIC) with a 2.8dB insertion-loss at 1550nm. This insertion loss is just 1.0dB higher than for a standard Fiber-to-PIC grating-coupler, and is due to a combination of interface-reflections and aberration-effects from the micro-optical elements in the MOB. We use further 2D-FDTD simulations to investigate the alignment and manufacturing tolerances of the MOB, and show that these are compatible with practical photonic-packaging processes for mass-manufacture.**

***Index Terms*—Integrated circuit packaging, Laser applications, Optical fibers.**

I. Introduction

A re-deployment of complementary metal oxide semiconductor (CMOS) technologies, which were developed and optimized for the electronics industry, for photonic applications has created a credible route to mass-manufacturable Si-photonic devices to address communications and sensing mass-markets [1, 2]. In addition, the growing availability of multi-project wafer (MPW) photonic-foundry services, which offer a rich catalogue of passive and active building-blocks, has served to de-risk the design and fabrication of photonic integrated circuits (PICs). In addition, the high refractive-index contrast of the silicon-on-insulator (SOI) platform allows for very small photonic components, which means that many devices can be harvested from a single dedicated SOI-wafer, e.g. 10^4 (2mm × 2mm) devices can be realized on a 300mm wafer [3].

While Fiber-to-PIC edge- and grating-coupling are often useful means of delivering light to the SOI-PIC, for certain applications an on-PIC light-source is preferred, especially in the medical- and sensing-spaces, where (i) there is often no need to integrate the photonic device into telecom or datacom fiber-network and (ii) having a small and handy packaged device with its own embedded source is vital.

Manuscript submitted August 12, 2018. This work was supported by Science Foundation Ireland (SFI) under Grant 12/RC/2276.

L. Zagaglia, F. Floris, L. Carroll, and P. O'Brien are with the Tyndall National Institute, Lee Maltings, Cork, Ireland, (luca.zagaglia@tyndall.ie).

Given that Si is an indirect band-gap material, it is not trivial to develop an efficient intrinsic, or monolithically-grown, light-source on the SOI-platform.

Different schemes for heterogeneous integration of III-V materials on SOI have been demonstrated, such as transfer-printing [4] or wafer-bonding [5, 6] and hybrid laser-integration can also be efficient and cost-effective due to a better scalability giving a further advantage for mass markets. In the hybrid approach, a stand-alone "known good" laser-diode is opto-mechanically coupled to the SOI-PIC, using either an edge-coupling scheme [7], micro-optic coupling to gratings [8, 9], or direct chip-to-chip coupling to gratings [10]. In the case of grating-coupling, a micro-optical bench (MOB) can be used to match the mode-field diameter (MFD) and numerical aperture (NA) of the diffraction-limited laser-diode emission to that of the approximately 10μm × 10μm acceptance-footprint of standard SOI grating-couplers available from the photonic-foundries. The MOB acts to relax hybrid laser-integration alignment tolerances to approximately ±2.5μm (1dB) [11], which is compatible with practical manufacturing and photonic-packaging processes [12].

In this paper, we show how millimeter-scale two dimensional finite difference time domain (2D-FDTD) simulations can be used to capture the full physics of laser hybrid-integration on the SOI-platform, which consists of (i) the propagation of the laser-mode through the micro-optics of the MOB, and (ii) the diffraction of the MOB-mode, incident on the grating-coupler, into the waveguides of the SOI-PIC, all in a single-shot simulation. These simulations allow the whole laser-to-waveguide insertion-loss to be calculated, and compared to that of a standard Fiber-to-PIC grating-coupler. Despite the spherical-aberration introduced by the micro-lens and the interface-reflections from the micro-lens and micro-prism in the MOB, a Laser-to-PIC total insertion-loss of 2.8dB is possible, which is just 1dB higher than the Fiber-to-PIC insertion-loss, using exactly the same grating-coupler design. Further 2D-FDTD simulation campaigns are used to investigate the alignment and manufacturing tolerances of the MOB, and the results indicating that they are compatible with practical photonic-packaging processes, such as UV-curing gluing, flip-chip and precision PIC and place.

II. MOB Design and Simulation

Fig. 1(a) shows a scheme of Fiber-to-PIC, and MOB-based Laser-to-PIC coupling.

Standard grating-couplers available from the process design kits (PDKs) of the photonics foundries are designed to accept

This article has been accepted for publication in a future issue of this journal, but has not been fully edited. Content may change prior to final publication. Citation information: DOI 10.1109/LPT.2018.2883211, IEEE Photonics Technology Letters

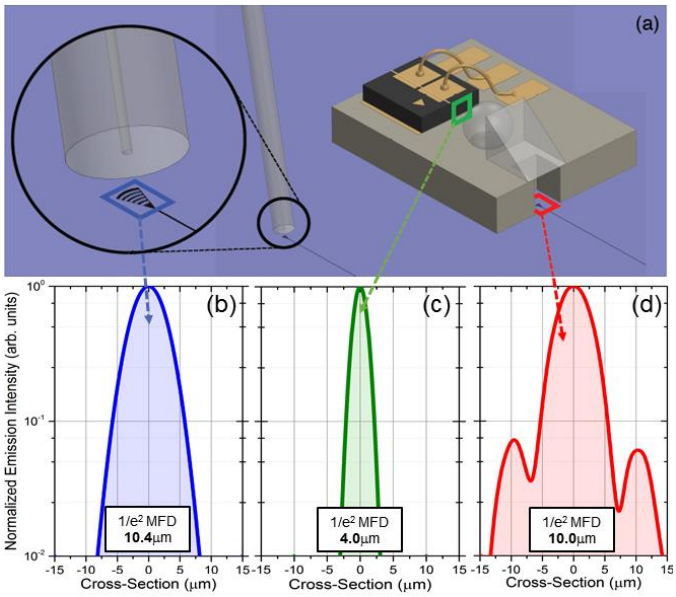

Fig. 1. (a) Comparison between a vertical single mode fiber and the MOB systems. (b) Cross section of the Gaussian-intensity emission profile emitted by a single mode fiber, which has typically a mode field diameter of 10.4μm. (c) Cross section of the Gaussian source intensity profile used as laser light source (d) Cross section along a perpendicular direction respect to the light propagation of the 2D-FDTD MOB focal spot taken at the most intense region.

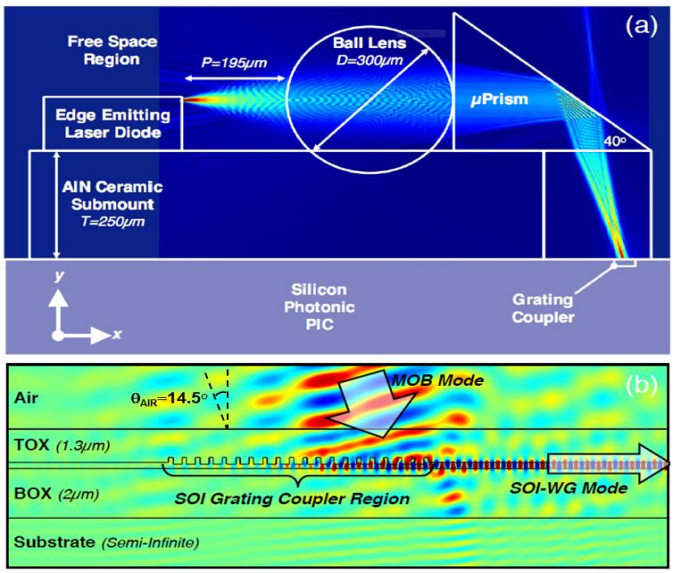

Fig. 2. (a) Light propagation inside the 2D FDTD simulation region. (b) Diffraction of the MOB mode inside the 220nm WG through the GC.

emission intensity profile with a MFD of 10.4μm, which is the benchmark used to model the fiber emission through a Gaussian source in the 2D-FDTD simulation - see Fig. 1(b). These standard grating-couplers are not well-matched to accept the beam-profile from a typical laser-diode, which has a diffraction-limited emission from a waveguide region with a typical cross-section on the order of 2 μm × 1 μm - see Fig. 1(c). The micro-optics of the MOB act to facilitate mode-matching between the laser-diode and the grating-coupler in two ways - (i) the ball-lens images the laser-mode on the grating-coupler with the required 10μm–MFD - see Fig. 1(d), and (ii) the micro-prism ensures that the imaged laser-mode is incident on the grating-coupler with the required angle-of-incidence (AOI) of approximately 10°.

Fig. 2(a) shows the design-parameters of our simulated MOB – (i) a 110 μm thick laser-diode with full-angle ($1/e^2$) vertical-divergence of 28° [13], (ii) a 300μm- diameter fused-silica (n_{FS} = 1.44) ball-lens, (iii) a 300μm-height fused-silica micro-prism, polished to a 40° angle, and (iv) a 250 μm -thick AlN-ceramic sub-mount with a cut-out below the prism to allow the re-imaged laser-mode access to the grating- coupler on the SOI-PIC. These design-parameters are typical of a existing MOB designs [9].

The design-parameters of the grating-coupler in our simulations are – (i) a 220nm SOI-layer, (ii) a 160nm poly-Si overlay, (iii) a 230nm etch-depth, i.e. the full poly-Si overlay, plus 70nm of the SOI-layer, (iv) a 30% duty-cycle, (v) a 2.0μm bottom-oxide layer (BOX), and (vi) a 1.3μm top-oxide layer (TOX) – see Fig. 2(b). These parameters are known to be the basis for the standard 1550nm TE-polarized grating-couplers, designed for an angle-of-incidence (AOI) of 10° that are offered by the IMEC MPW Si-Photonic foundry service [14]. Ray-tracing software, such as *Zemax*™ [15], is typically used to model light-propagation through micro-optic systems, like the MOB [9]. However, these ray-tracing models use geometric-optic rules and empirical algorithms, rather than a true physics-engine, to generate solutions. In this work, we exclusively use 2D-FDTD simulations to optimize the MOB design, evaluate the Laser-to-PIC insertion-loss, and determine the alignment and manufacturing tolerances. An FDTD simulation makes no underlying assumptions or simplifications about the micro-optic elements in the MOB or the properties of the grating-coupler; it simply propagates light through the designate simulation-space in accordance with Maxwell's equations. As a result, the accuracy of a properly defined FDTD simulation depends only on how finely "meshed" is the simulation-space, which is practically limited only by the memory and processing speed of the computer running the simulation. We used commercially available *Lumerical* ® FDTD Solutions™ [16] to run millimeter-scale 2D-FDTD simulations, to capture the full physics of the laser-mode propagation through the micro-optics of the MOB, and the diffraction at the grating-coupler, in order to evaluate the Laser-to-PIC Insertion Loss (IL) - see Fig 2.

A convergence test identified the minimum meshing-density needed for the simulations, and an auto-generated non-uniform mesh (on the order of 30nm × 30nm at the grating-coupler, and 80nm × 80nm at the micro-lens) was found to be adequate. The 850μm × 550μm 2D-FDTD simulation used to describe the MOB takes 3 hours to run on a PC with a liquid-cooled 16-core processor and 64GB of RAM. Clearly, this large 2D-FDTD simulation captures only the divergence of the laser-diode and the focusing-effect of the micro-lens in the x-y plane, but these are the parameters that most directly affect the Laser-to-PIC IL value, because they determine the phase-front of the focused mode *across* the diffractive-elements of the grating-coupler [17]. In contrast, divergence and focusing in

This article has been accepted for publication in a future issue of this journal, but has not been fully edited. Content may change prior to final publication. Citation information: DOI 10.1109/LPT.2018.2883211, IEEE Photonics Technology Letters

the "missing" x-z plane of the 2D-FDTD simulation only affects the size of the focused mode *along* the diffractive-elements of the grating-coupler, which can be easily managed by tuning the width of the coupler.

As shown in Fig. 2, light is "injected" into the 2D-FDTD simulation from a Gaussian-mode source with a MFD and NA consistent with that of a commercial laser-diode [13], propagates through the micro-optic ball-lens, undergoes total internal reflection (TIR) at the polished-facet of the micro-prism, exits and refracts at the bottom-facet of the micro-prism with an angle of $\theta_{AIR} = 14.5°$, and is focused onto the TOX-layer of the PIC, where it undergoes a second refraction effect to be incident on the grating-coupler with an AOI of $\theta_{GC} = 10°$. To facilitate passive-alignment during its fabrication, the MOB design calls for the micro-prism to be pushed into physical contact with the ball-lens.

To reduce manufacturing costs, the MOB design should also use a "standard" AlN ceramic thickness, i.e. 250µm. As a consequence, the only design-parameter that can be used to tune the size of the focused-mode on the grating coupler is the Laser-to-Lens distance (P). A series of 2D-FDTD simulations were used to identify the value of P that offered the best Laser-to-PIC insertion-loss for the above MOB design. As shown in Fig. 3(a), the optimum MOB design, with P = 195µm, offers an insertion-loss of 2.8dB at 1550nm with a standard grating-coupler.

III. MOB Insertion Losses and Tolerances

Fig. 3(a) compares the spectra of both Fiber-to-PIC and Laser-to-PIC coupling using identical standard grating-couplers.

Fiber-to-PIC coupling offers an insertion-loss of 1.8dB at the target wavelength of 1550nm, indicating an MOB performance-penalty of 1.0dB. Thanks to our millimeter-scale 2D-FDTD simulation, able to capture the whole physics behind aberration, reflection and diffraction in the light propagation in the MOB, we can attribute this approximately 20% reduction in coupling to two effects: (i) reflections at the multiple air-to-glass interfaces for about 12%, and (ii) reduced modal-overlap of the focused-mode on the grating-coupler due to spherical-aberration effects for around 8%.

The losses from interface-reflections can be easily minimized by using suitable anti-reflection coatings while designing a grating-coupler that can accommodate the extended spot-size and variable phase-front of the spherically-aberrated focused mode will be more challenging. However, the same particle swarm optimization and genetic-algorithm techniques that have been successfully used to develop chirped and apodized grating-couplers can likely be repurposed to this task [18, 19].

The Laser-to-PIC coupling spectrum in Fig. 3(a) is for a perfectly fabricated MOB that is perfectly aligned over the grating-coupler. To investigate the alignment tolerances of the MOB, and compare them to direct Fiber-to-PIC coupling, a campaign of 2D-FDTD simulations were used, in which horizontal (Δx) and vertical (Δy) offsets were applied to the ideal MOB (and fiber) positions.

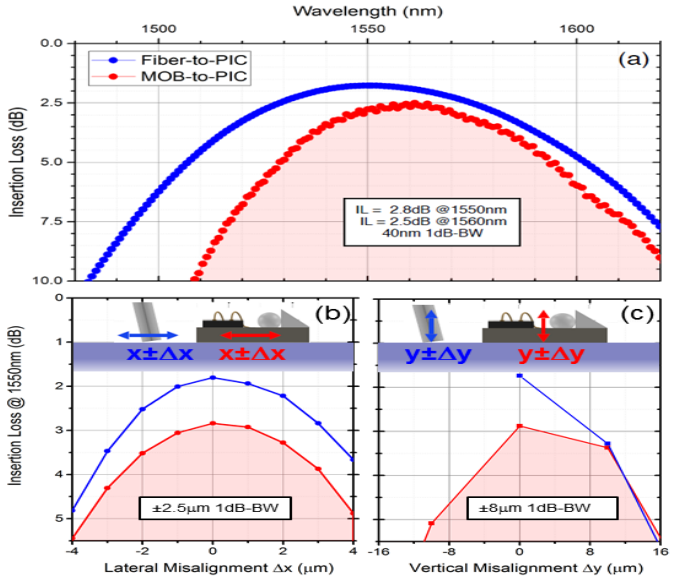

Fig. 3. (a) A comparison between the IL of the Fiber-to-PIC system and the MOB-to-PIC. The blue line refers to the Fiber's IL and the red one refers to the MOB. (b,c) Comparisons in the IL between the lateral and vertical misalignments for the Fiber-to-PIC and MOB-to-PIC systems, Δx and Δy respectively, with respect to their corresponding best positions x and y.

Fig. 3(b) shows that both the MOB and Fiber have a comparable 1dB horizontal alignment tolerance of ±2.5µm, which is compatible with epoxy-bonding of the MOB to the surface of the PIC, after an active-alignment step. The 1dB limit in the tolerances is considered being the benchmark for alignment processes in packaging.

Fig. 3(c) shows that the MOB has a 1dB vertical alignment tolerance of ±8µm, which is outside the ±5% manufacturing tolerances that are typical for a 250µm-thick AlN-substrate. However, it is always possible to re-align along the x-direction the GC compensating the wrong impinging position taking advantage of the extended MOB-focal region (i.e. 65µm). Note that the Fiber-to-PIC alignment data are only shown for positive values of Δy, because the fiber cannot be pushed "through" the PIC surface. These results show that the 1dB alignment tolerances of the MOB are similar to those of a fiber for grating-coupling, and are compatible with existing practical alignment processes.

Fig. 4 illustrates the effect of fabrication tolerances on the MOB coupling performances. A campaign of 2D-FDTD simulations were used to investigate the effect of an horizontal offset (ΔP) affecting the laser best horizontal position (P) and a vertical offset (ΔQ) affecting the micro-lens best vertical position (i.e. Q=0µm, so the lens optical-axis is properly aligned with respect to the laser exit slit - see Fig 2(a)).

Fig. 4(a) shows that 1dB laser-to-lens horizontal alignment tolerance is ±20µm, which is well within the capabilities of either flip-chip or precision pick-and-place processes for attaching the laser-diode to the AlN-substrate. Fig. 4(b) shows that 1dB laser-to-lens vertical alignment tolerance is significantly tighter, at +5 µm /-15 µm. The asymmetry in this tolerance is due to the fact that a symmetric ±ΔQ results in an

This article has been accepted for publication in a future issue of this journal, but has not been fully edited. Content may change prior to final publication. Citation information: DOI 10.1109/LPT.2018.2883211, IEEE Photonics Technology Letters

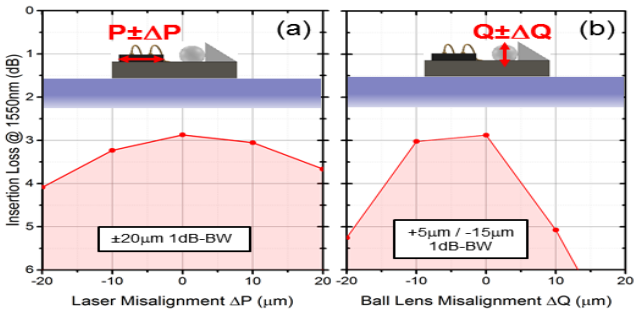

Fig. 4. (a) Behavior of the IL value due to a laser misalignment on the ceramic substrate. b) Variation in the IL as a function of a misalignment in the ball lens height. (a) and (b) represent the consequences in the IL value of the fabrication tolerances.

asymmetric change in both the optical path-length and propagation-direction through the micro-prism.

It also changes the AOI of the focused-mode arriving at the surface of the PIC, and displaces the focused-mode across the grating-coupler. To compensate for this last effect, the horizontal position of the MOB above the grating-coupler (i.e. x) is re-adjusted for each data-point in Fig. 4(b), so that the results are shown under conditions of optimum alignment.

In practice, there are two potential origins of ΔQ offsets – (i) a variation in the thickness of the laser-diode, due to the InP-wafer polishing-tolerances, and (ii) a variation in the width of the micro-lens locating-hole/slot on the AlN-substrate, due to fabrication tolerances. According to the manufacturing tolerances reported in [9], the -15μm 1dB alignment tolerance is technically within the variations introduced by this effect, even though the margin is rather tight; however, the +5 μm 1dB alignment tolerance is outside of the manufacturing tolerances, around 12 μm. Therefore, not only care must be taken to ensure that these components are manufactured to a high-degree of their nominal specification, but also improvements in the fabrication processes must be introduced.

The difference of 1.0dB in the IL of the Fiber-to-PIC and MOB-to-PIC coupling can be divided into two different contributions the light back reflected at each surface of the optical components (0.6dB), which can be eliminated with suitable anti-reflective coatings, and the spherical-aberration (0.4dB), which can be accommodated through custom non-uniform grating-couplers. This suggests that the MOB can potentially be a reasonable alternative to the fiber in order to couple light directly into a PIC. However, it is to be considered that a full 3D model is needed to capture the entire complexity of the real MOB features.

IV. Conclusion

Millimeter-scale 2D-FDTD simulations are demonstrated to be a practical solution for optimizing MOB designs for efficient Laser-to-PIC hybrid integration. Compared to direct Fiber-to-PIC coupling, a basic MOB suffers from a performance-penalty of just 1.0dB compared to a fiber-coupling. Both alignment and manufacturing tolerances of the MOB are shown to be compatible with practical photonic-packaging processes.

V. References

[1] M. Streshinsky, R. Ding, Y. Liu, A. Novack, C. Galland, A. Lim, P. Guo-Qiang Lo, T. Baehr-Jones, and M. Hochberg, "The road to affordable, large-scale silicon photonics," Opt. Photon. News, vol. 24, no. 9, pp. 32–39 , Sept. 2013, DOI: 10.1364/OPN.24.9.000032

[2] L. Tsybeskov, D.J. Lockwood, and M. Ichikawa, "Silicon photonics: CMOS going optical," Proceedings of the IEEE, vol. 97, no. 7, pp. 1161–1165, July 2009, DOI: 10.1109/JPROC.2009.2021052.

[3] Si-Photonics at EuroPractice - www.europractice-ic.com/SiPhotonics_technology.php

[4] R. Loi, J. O'Callaghan, B. Roycroft, C. Robert, A. Fecioru A. J. Trindade, A. M. Gocalinska, C. A. Bower, and B. M. Corbett, "Transfer printing of AlGaInAs/InP etched facet lasers to Si substrates," IEEE Photonics J., vol. 8, no. 6, pp. 1–10, Dec. 2016, DOI: 10.1109/JPHOT.2016.2627883.

[5] B. B. Bakir, C. Sciancalepore, A. Descos, H. Duprez, D. Bordel, L. Sanchez, C. Jany, K. Hassan, P. Brianceay, V. Carron, and S. Menezo, "Heterogeneously integrated III-V on silicon lasers," ECS Transaction, vol. 64, no. 5, pp. 211–223, 2014, DOI: 10.1149/06405.0211ecst.

[6] B. Corbett, C. Bower, A. Fecioru, M. Mooney, M. Gubbins, and J. Justice, "Strategies for integration of lasers on silicon," Semicond. Sci. Technol., vol. 28, no. 9, pp. 1–6, 21 Aug. 2013, DOI: 10.1088/0268-1242/28/9/094001.

[7] J. H. Lee, I. Shubin, J. Yao, J. Bickford, Y. Luo, S. Lin, S. S. Djordjevic, H. D. Thacker, J. E. Cunningham, K. Raj, X. Zheng, and A. V. Krishnamoorthy, "High power and widely tunable Si hybrid external-cavity laser for power efficient Si photonics WDM links," Opt. Express, vol. 22, no. 7, pp. 7678–7685, 26 Mar 2014, DOI:10.1364/OE.22.007678.

[8] P. De Dobbelaere, "External source approach for silicon photonics transceivers," 40th ECOC, Cannes, F, Sept. 2014, Available: http://www.ecoc2014.org/uploads/Workshops/WS1/ECOC2014_WS1_Peter%20De%20Dobbelaere.pdf

[9] B. Snyder, B. Corbett, and P. O'Brien, "Hybrid integration of the wavelength-tunable laser with a silicon photonic integrated circuit," J. Lightwave Technol., vol. 31, no. 24, pp. 3934–3942, 15 Dec. 2013, DOI: 10.1109/JLT.2013.2276740.

[10] B. Song, L. Megalini, S. Dwivedi, S. Ristic, and J. Klamkin, "High-Thermal Performance 3D Hybrid Silicon Lasers," IEEE Photon. Technol. Lett., vol. 29, no. 14, pp. 1143-1146, 15 Jul. 2017, DOI: 10.1109/LPT.2017.2702593.

[11] L. Carroll, J. S. Lee, C. Scarcella, K. Gradkowski, M. Duperron, H. Lu, Y. Zhao, C. Eason, P. Morrissey, M. Rensing, S. Collins, H. Y. Hwang, and P. O'Brien, "Photonic Packaging: Transforming silicon photonic integrated circuits into photonic devices," Appl. Sci., vol. 6. no. 12, pp. 1-21, 15 Dec. 2016, DOI: 10.3390/app6120426.

[12] M. Duperron, L. Carroll, M. Rensing, S. Collins, Y. Zhao, Y. Li, R. Baets, and P. O'Brien, "Hybrid integration of laser source on silicon photonic integrated circuit for low-cost interferometry medical device," in SPIE OPTO, San Francisco, CA, USA, 2017, pp. 1–18.

[13] H. Sun, "Laser Diode Beam Basics" in A Practical Guide to Handling Laser Diode Beams, 1st ed. Pittsburgh, PA, USA: Springer, 2015, ch. 2., sec. 2.1.2, pp 28–29, DOI: 10.1007/978-94-017-9783-2_1.

[14] G. Roelkens, D. V. Thourhout, and R. Baets, "High efficiency Silicon-on-Insulator grating coupler based on a poly-Silicon overlay," Opt. Express, vol. 14, no. 24, pp. 11622–11630, 27 Nov. 2006, DOI: 10.1364/OE.14.011622.

[15] Zemax LLC. https://www.zemax.com/products/opticstudio/

[16] Lumerical Inc. http://www.lumerical.com/tcad-products/fdtd/

[17] D. Vermeulen, S. Selvaraja, P. Verheyen, G. Lepage, W. Bogaerts, P. Absil, D. Van Thourhout, and G. Roelkens, "High-efficiency fiber-to-chip grating couplers realized using an advanced CMOS-compatible Silicon-On-Insulator platform," Opt. Express, vol. 18, no. 17, pp. 18278–18283, 16 Aug. 2010, DOI: 10.1364/OE.18.018278.

[18] R. Marchetti, C. Lacava, A. Khokhar, X. Chen, I. Cristiani, D. J. Richardson, G. T. Reed, P. Petropoulos, and P. Minzioni, "High-efficiency grating-couplers: demonstration of a new design strategy," Sci. Rep., vol. 7, no. 16670, pp. 1–8, 30 Nov. 2017, DOI:10.1038/s41598-017-16505-z.

[19] A. Bozzola, L. Carroll, D. Gerace, I. Cristiani, and L. C. Andreani, "Optimising apodized grating couplers in a pure SOI platform to -0.5 dB coupling efficiency," Opt. Express, vol. 23, no. 12, pp. 16289–16304, 15 Jun 2015, DOI:10.1364/OE.23.016289G.